Journal of Power Sources 223 (2013) 79–85

Contents lists available at SciVerse ScienceDirect

Journal of Power Sources

journal homepage: www.elsevier.com/locate/jpowsour

Improvement in stability of carbon support for platinum catalyst by applying silicon carbide coating

Shuichi Suzuki*, Taigo Onodera, Jun Kawaji, Takaaki Mizukami, Makoto Morishima, Kenji Yamaga

Hitachi Research Laboratory, Hitachi, Ltd., 7-1-1 Omika-cho, Ibaraki 319-1292, Japan

HIGHLIGHTS

- We prepared silicon-carbide-coated carbon black for support material of platinum.
- The support material was synthesized by pyrolyzing polycarbosilane.
- Oxygen reduction activity was increased using the support material.
- Catalyst stability was improved using the support material.

GRAPHICAL ABSTRACT

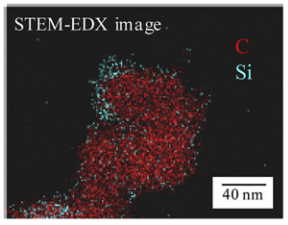

Silicon–carbide–coated carbon black (SiC/C)

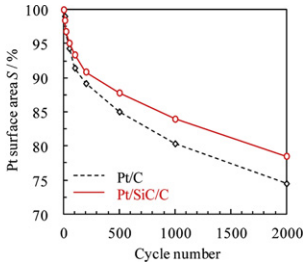

ARTICLE INFO

Article history:
Received 1 May 2012
Received in revised form
27 July 2012
Accepted 14 September 2012
Available online 21 September 2012

Keywords:
Silicon carbide
Carbon support
Stability
Oxygen reduction reaction
Fuel cell

ABSTRACT

Silicon-carbide-coated carbon blacks (SiC/C) were investigated as support materials of platinum (Pt) nanoparticles to improve their stability. The support materials were synthesized by pyrolyzing the mixture of polycarbosilane and carbon blacks. An elemental mapping image of the support material showed that the carbon black was coated with a layer of silicon carbide less than 10 nm thick. Both the electric resistance and surface area of the support materials were of the same order as the carbon black only. The platinum nanoparticles were deposited on the support materials by electroless plating. The oxygen reduction activity of the catalysts was measured electrochemically using a rotating disk electrode. The measurement showed that the specific activity of the catalyst increased when silicon carbide was added. The catalyst stability was evaluated using thermogravimetric (TG) analysis in air from room temperature to 1273 K and potential-cycling test between 1.0 and 1.5 V. These results revealed that the catalyst stability of Pt/SiC/C was higher than that of Pt/C. This high stability of Pt/SiC/C is attributed to the protective effect of SiC against carbon corrosion that is enhanced by the platinum nanoparticles.

1. Introduction

Polymer electrolyte fuel cells (PEFCs) are promising power sources for automotive and stationary applications due to their low pollutant emission and high energy-conversion efficiency. PEFCs have been intensively developed for decades to their performance, but a longer lifetime is still needed before extensive commercialization is possible. Cathode catalysts are mainly composed of platinum nanoparticles on a carbon support, and catalyst degradation is one of the main factors that reduce the lifetime of PEFCs [1,2]. One of main causes of catalyst degradation is loss of the platinum surface area due to corrosion of the carbon supports and subsequent agglomeration of platinum nanoparticles [3]. Carbon supports, such as carbon black, are thermodynamically unstable and may corrode at the high potentials typical of PEFC cathodes [4,5]. In addition, the carbon corrosion is accelerated by the catalytic effect of platinum nanoparticles on the carbon support [6–8]. Therefore, an alternate support material is needed to improve the stability of the cathode catalyst.

* Corresponding author. Tel.: +81 294 52 5111; fax: +81 294 52 7624.
E-mail address: shuichi.suzuki.fw@hitachi.com (S. Suzuki).

0378-7753/$ – see front matter © 2012 Elsevier B.V. All rights reserved.
http://dx.doi.org/10.1016/j.jpowsour.2012.09.042

Ceramic materials such as titanium oxide (TiO_2, Ti_4O_7) [9–13], niobium-doped titanium oxide (Nb–TiO_2) [14,15], niobium oxide (NbO_2) [16], tin oxide (SnO_2) [13,17,18], tantalum oxide (Ta_2O_5) [13,19], zirconium oxide (ZrO_2) [13], tungsten oxide (WO_3) [13,20,21], titanium nitride (TiN) [22,23], tungsten carbide (WC) [24], and silicon carbide (SiC) [25] have recently come to be regarded as promising support materials because they are more stable in the high-potential condition relative to the carbon. On the other hand, the ceramic materials are generally inferior to carbon in electrical conductivity. Furthermore, it is difficult to synthesize the ceramic materials with a large surface area to obtain highly dispersed platinum nanoparticles.

SiC coated carbon nanotubes have been reported to demonstrate high oxidation resistance [26,27]. This material is thought to show higher electrical conductivity than ceramic particles because the carbon core can serve as an electron path. The material is additionally expected to have a large surface area because of the reflective morphology of the carbon core. Furthermore, we previously reported that the ceramic supports enhance the platinum catalytic activity compared to the carbon supports [28]. Therefore, SiC coated carbon is one of the most promising support materials.

In this work, we investigated SiC coated carbon black (SiC/C) used as the support material for platinum nanoparticles to improve the stability of the cathode catalyst. The SiC/C was synthesized using pyrolysis of polycarbosilane (PCS) on the carbon black. The platinum nanoparticles were deposited on the SiC/C using an electroless plating method. The oxygen-reduction activity of the catalyst was measured in a perchloric acid ($HClO_4$) solution. The catalyst stability was evaluated from the weight loss of the catalyst using thermogravimetric (TG) analysis under air from room temperature to 1273 K. The stability was also evaluated by potential–cycling test between 1.0 and 1.5 V in the $HClO_4$ solution at 337 K.

2. Experimental

2.1. Preparation and characterization of SiC/C

The synthesis of SiC/C was carried out by using pyrolysis of PCS [29]. Either 0.3 or 1.2 g of PCS dissolved in 2.4 g of hexane and 3.2 g of octylphenol polyethyleneglycol ether were added to 200 mL of water. Then, the solution was stirred and ultrasonically dispersed for 1 h at room temperature. Then 2.0 g of carbon black (Cabot corp.; Vulcan XC-72R) was added to the solution, and it was further stirred for 4 h at room temperature. After that, the PCS-carbon black mixture was filtered and washed with water. Then the mixture was cured at 493 K for 12 h in air. Finally, the mixture was heated at 1173 K for 3 h under argon in order to pyrolyze the PCS into SiC. The weight ratios of PCS to carbon black (PCS/C) in this synthesis were 0.15 and 0.60, and the supports were named SiC/C-1 and SiC/C-2, respectively. The carbon black without SiC was also used, and it was named C-1.

The amount of SiC in the support materials was calculated from the remaining weight after burning the support materials with a TG analyzer (TG/DTA-6200; Seiko Instruments Inc.). The burning condition was under air from room temperature to 1273 K at a heating rate of 10 K min^{-1}. The surface area of the support material was evaluated with the Brunauer-Emmett-Teller (BET) method using nitrogen desorption isotherms (AUTOSORB-1; Quantachrome Corp.). The electrical conductivity of the support material powder was measured by filling a PTFE cylinder with a 1-cm^2 hole with the powder and then applying 28 MPa of pressure with stainless electrodes. The morphology of SiC on carbon black was observed using scanning transmission electron microscopy (STEM) (Hitachi Ltd.; HD-2700) coupled with energy dispersive X-ray spectroscopy (EDX) (EDAX Inc.; Genesis). The chemical state of Si in the SiC was analyzed using X-ray photoelectron spectroscopy (XPS) (ULVAC-PHI Inc.; PHI 5000). The crystallographic structure of the SiC was analyzed by using an X-ray diffractometer (XRD) (Rigaku Corp.; RU-200BH) with Cu*Ka* radiation.

2.2. Preparation and characterization of catalysts

The platinum nanoparticles on C-1, SiC/C-1, and SiC/C-2 were synthesized by electroless plating [30,31]. Hydrogen hexachloroplatinate (IV) solution (H_2PtCl_6; [Pt] = 28.2 wt.%) was used as a platinum precursor. L-tartaric acid, hypophosphite solution (H_3PO_2; 50 wt.%), and sodium hydroxide solution (NaOH; 1 mol L^{-1}) were used as a chelate ligand, a reducer, and a pH adjuster, respectively. The support material was added to 200 ml of aqueous solution, and this was stirred for 1 h at room temperature. The added amount of the support material was 0.50 g (C-1), or 0.53 g (SiC/C-1), or 0.73 g (SiC/C-2); the amount was determined in order to achieve a uniform amount of carbon black in the support materials. Then, H_2PtCl_6 (2.57 mmol) and L-tartaric acid (0.26 mmol) were added to the solution, which was further stirred for 1 h at room temperature. Next, H_3PO_2 (5.14 mmol) was added to the solution. The pH of the solution was then adjusted to 4 by adding NaOH, and the total volume of solution was set to 500 ml by adding water. After that, the solution was stirred at 363 K for 4 h. Finally, the obtained catalysts were washed with water and dried at 353 K under air for 12 h. The catalysts using the support materials of C-1, SiC/C-1, and SiC/C-2 were named Pt/C-1, Pt/SiC/C-1, and Pt/SiC/C-2, respectively.

The loading amount of the platinum nanoparticles was evaluated using the following procedure. The platinum nanoparticles were firstly dissolved by alkali fusion method with sodium peroxide and sodium carbonate. After that, it was dissolved with hydrochloric acid, and the amount of platinum in the solution was analyzed by using inductively coupled plasma (ICP) (Horiba Ltd.; ULTIMA-2). The morphology of the platinum particles was observed by using STEM. The crystallographic structure of the platinum was analyzed by using XRD.

2.3. Evaluation of oxygen reduction activity

The platinum surface area and oxygen-reduction activity of the catalysts were measured electrochemically using a rotating disk electrode (RDE). The working electrode was created using the following procedure. The catalysts were first ultrasonically dispersed in water (0.1 mg ml^{-1}). 20 μL volume of the catalyst solution was then pipetted onto an RDE (made of glassy carbon with a disk surface area of 0.2 cm^2), yielding a catalyst loading of 0.2 mg cm^{-2}. After drying the RDE, 4 μL volume of 0.1 wt% Nafion® diluted with a mixed solution of iso-propanol and water (1:1 in wt %) was poured over the catalyst layer and dried to fix the catalyst. A platinum wire was used as the counter electrode. A reversible hydrogen electrode (RHE) was used as the reference electrode, and all potentials throughout this paper are referenced to the RHE.

Prior to measuring of the oxygen-reduction activity, the potential of the working electrode was cycled 30 times between 0.03 and 1.2 V at 0.2 V s^{-1} in 0.1 mol L^{-1} $HClO_4$ under an atmosphere saturated with nitrogen at 308 K in order to clean the surface and allow the surface area to be measured. The surface area was calculated from the electric charge of hydrogen adsorption and desorption in the data from the 30th potential sweep. A conversion value of 0.21 mC cm^{-2} was used for the calculation.

The oxygen-reduction current was measured in 0.1 mol L^{-1} $HClO_4$ saturated with oxygen at 308 K. The potential of the working electrode was swept from 1.1 V to 0.2 V at 0.01 V s^{-1}. The working

Table 1
Description of support materials, PCS/C ratio in synthesis, SiC loading evaluated by TG, surface area measured by N_2 BET, and powder resistance.

Support material	PCS/C ratio in synthesis	SiC loading/wt. %	Surface area/$m^2\ g^{-1}$	Resistance/Ω cm
C-1	0	0	272	3.7×10^{-2}
SiC/C-1	0.15	11.8	196	5.9×10^{-2}
SiC/C-2	0.6	31.2	126	9.1×10^{-2}

electrode was rotated at a rate of 400–2500 rpm. The oxygen reduction current was calculated by subtracting the current measured under a nitrogen atmosphere from that under an oxygen atmosphere to remove any background current, and the oxygen-reduction activity was evaluated from the dependence of the rotation speed on the oxygen reduction current by using the Koutecky–Levich equation [32].

2.4. Evaluation of catalyst stability

The catalyst stability was evaluated from the weight loss of the catalyst using a TG analyzer (TG/DTA-6200; Seiko Instruments Inc.) under air from room temperature to 1273 K at a heating rate of 10 K min^{-1}.

The catalyst stability was also evaluated electrochemically by the potential-cycling test with periodic measurements of the platinum surface area. The measurement system was the same as that used for measuring the oxygen-reduction activity. In the cycling test, the potential of the working electrode was cycled 2000 times between 1.0 V and 1.5 V at 0.5 V s^{-1} in 0.1 mol L^{-1} $HClO_4$ saturated with nitrogen at 337 K. Cyclic voltammogram with a potential range from 0.03 to 1.2 V was measured during the cycling test to obtain the platinum surface area.

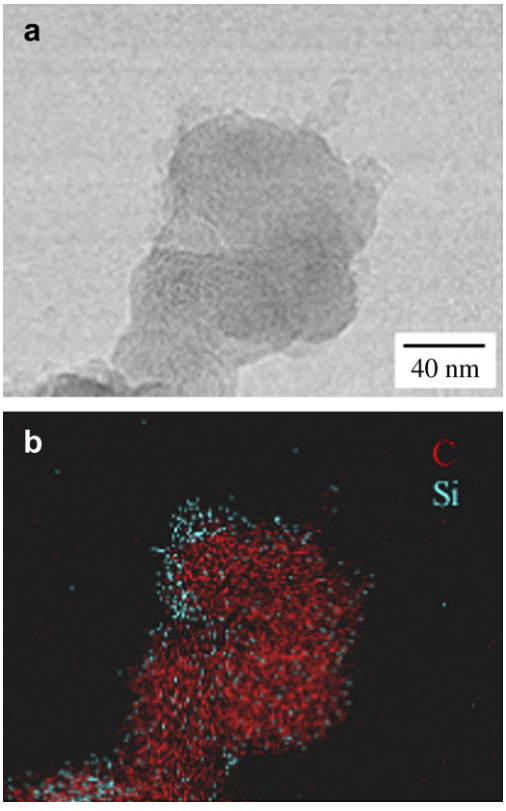

Fig. 1. Morphology of SiC/C-2; (a) STEM image, and (b) EDX elemental mapping image.

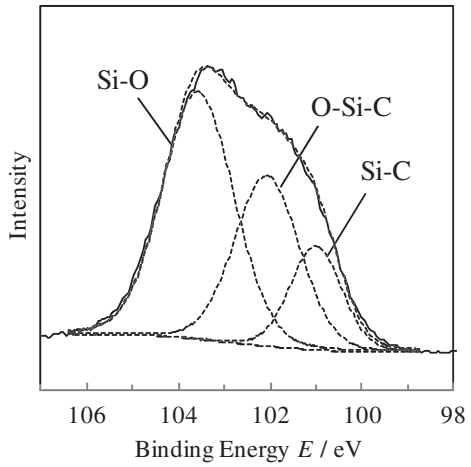

Fig. 2. Si 2p XPS profile of SiC/C-2.

3. Results and discussion

3.1. Characterization of support materials

Table 1 lists the SiC loading for the support materials as a function of the PCS ratio in the synthesis. The SiC loading increased with the increase in the PCS/C ratio. The yield of SiC from PCS was around 80% in weight. The STEM-EDX images of SiC/C-2 are shown in Fig. 1. The coating layer on the carbon black in the SiC/C-2 was less than 10 nm thick. According to the elemental mapping image, the layer contained silicon, indicating that the layer could be the SiC obtained from pyrolyzing the PCS. Agglomerates of SiC, which detached from the carbon black, were hardly observed in a low-magnification observation (not shown). The chemical state of Si in the SiC/C-2 was analyzed from Si 2p XPS (Fig. 2). The binding energy of Si–Si, Si–C, O–Si–C, and Si–O were reported as 99.2, 100.5, 101.8, and 103.2 eV, respectively [33]. The spectrum in Fig. 2 was decomposed into three peaks on the base of the reference. The state of Si–C was detected in the SiC/C-2 while that of Si–Si was not detected, meaning that the PCS was pyrolized into SiC. Furthermore, the states of O–Si–C and Si–O were also detected. This indicates that the surface of the SiC layer in SiC/C-2 was oxidized by oxygen in air. The XRD patterns of C-1 and SiC/C-2 were shown in

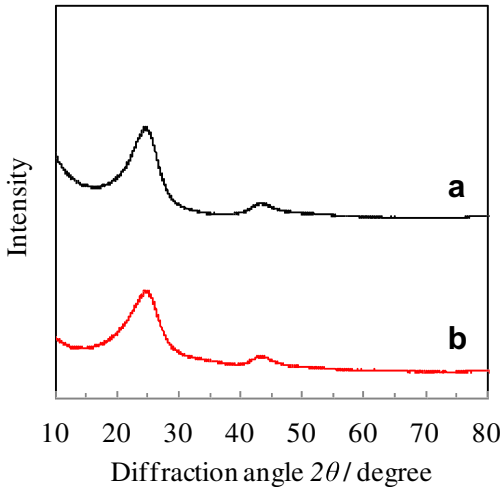

Fig. 3. XRD patterns of (a) C-1 and (b) SiC/C-2.

Table 2
Description of catalysts, Pt loading analyzed using ICP, Pt crystalline size evaluated from Pt (111) diffraction of XRD, Pt surface area measured by cyclic voltammogram, and oxygen reduction current at 0.9 V normalized by platinum weight and platinum surface area.

Catalyst	Pt loading/ wt. %	Pt crystalline size/nm	Pt surface area/$m^2\ g^{-1}$	Oxygen reduction current/ A g^{-1}-Pt@0.9 V	Oxygen reduction current/ μA cm^{-2}-Pt @ 0.9 V
Pt/C-1	46.0	2.3	62	42	67
Pt/SiC/C-1	44.8	2.6	57	51	89
Pt/SiC/C-2	39.8	4.1	34	46	136

Fig. 3. The pattern of SiC/C-2 was similar to that of C-1. The diffraction peaks around 25° and 43° can be indexed to the graphite (002) and (101) reflections, while peaks attributed to SiC crystal were not detected in the pattern of SiC/C-2. This fact indicates that the SiC in SiC/C-2 was amorphous.

The surface areas of the support materials are listed in Table 1. The surface area decreased as amount of SiC loading increased. The reason for the decrease in surface area is probably because the primary pores of the carbon black were filled with the SiC. However, more than 100 $m^2\ g^{-1}$ of surface area still remained in the SiC/C-2 with 31.2 wt. %-SiC. The electrical resistances of the powder support materials are listed in Table 1. Although the SiC coating caused an increase in the resistance of support materials, the resistances of the SiC/C-1 and SiC/C-2 were of the same order as that of the C-1 at 10^{-2} Ω cm. The resistance of SiC, which was synthesized without adding the carbon black, was also evaluated in this work. The value was 5.3×10^6 Ω cm, and it was significantly higher than those of SiC/C-1 and SiC/C-2. The low resistances of SiC/C-1 and SiC/C-2 resulted from the electrical path of the carbon black contained in the SiC/C-1 and SiC/C-2.

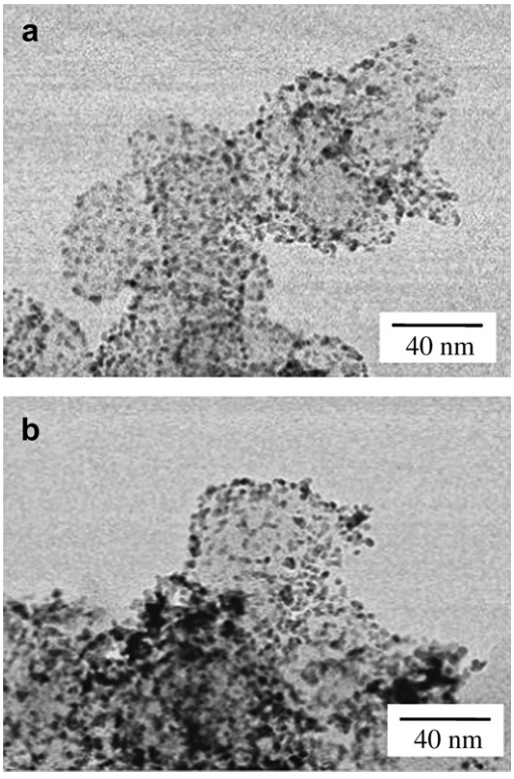

Fig. 4. STEM images of (a) Pt/C-1 and (b) Pt/SiC/C-2.

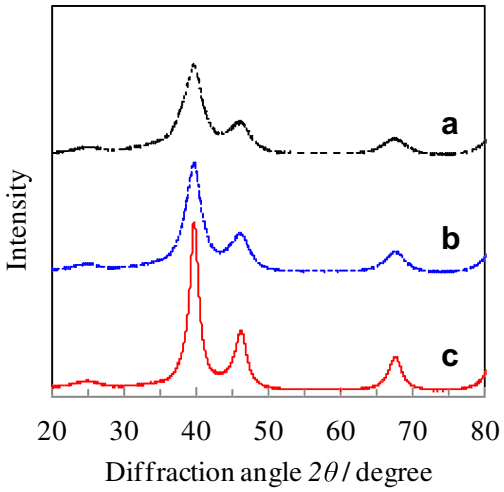

Fig. 5. XRD patterns of (a) Pt/C-1, (b) Pt/SiC/C-1, and (c) Pt/SiC/C-2.

3.2. Characterization of catalysts

Platinum loadings in the catalysts are listed in Table 2. In this work, the amount of platinum precursor added in the synthesis was decided in order to have a constant ratio of platinum to carbon black in all the catalysts. Therefore, the platinum loading was reduced as the amount of SiC was increased. The STEM images of platinum nanoparticles in the Pt/C-1 and Pt/SiC/C-2 are shown in Fig. 4. Platinum nanoparticles less than 5 nm were highly dispersed on each support material. However, the nanoparticles in Pt/SiC/C-2 were more agglomerated relative to those in Pt/C-1. The agglomeration of platinum nanoparticles in Pt/SiC/C-2 resulted from the small surface area of SiC/C-2 compared to that of the C-1. XRD patterns of all catalysts are shown in Fig. 5. All diffraction peaks are ascribed to the face-centered cubic (fcc) platinum. The diffraction peaks around 40, 46, and 67° can be indexed to the (111), (200), and (220) reflections. The crystalline sizes of the platinum, which were calculated from the diffraction peak of (111) using the Scherrer equation, are listed in Table 2. The crystalline size increased with the amount of SiC in the support materials. The crystalline size of Pt/SiC/C-2 (4.2 nm) was about twice as large as that of Pt/C-1

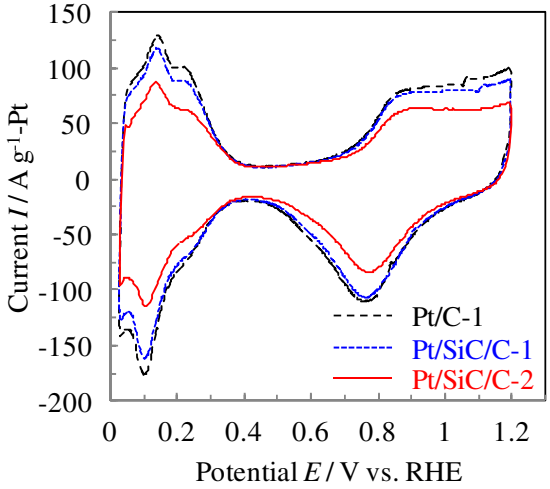

Fig. 6. Cyclic voltammograms of Pt/C-1, Pt/SiC/C-1, and Pt/SiC/C-2.

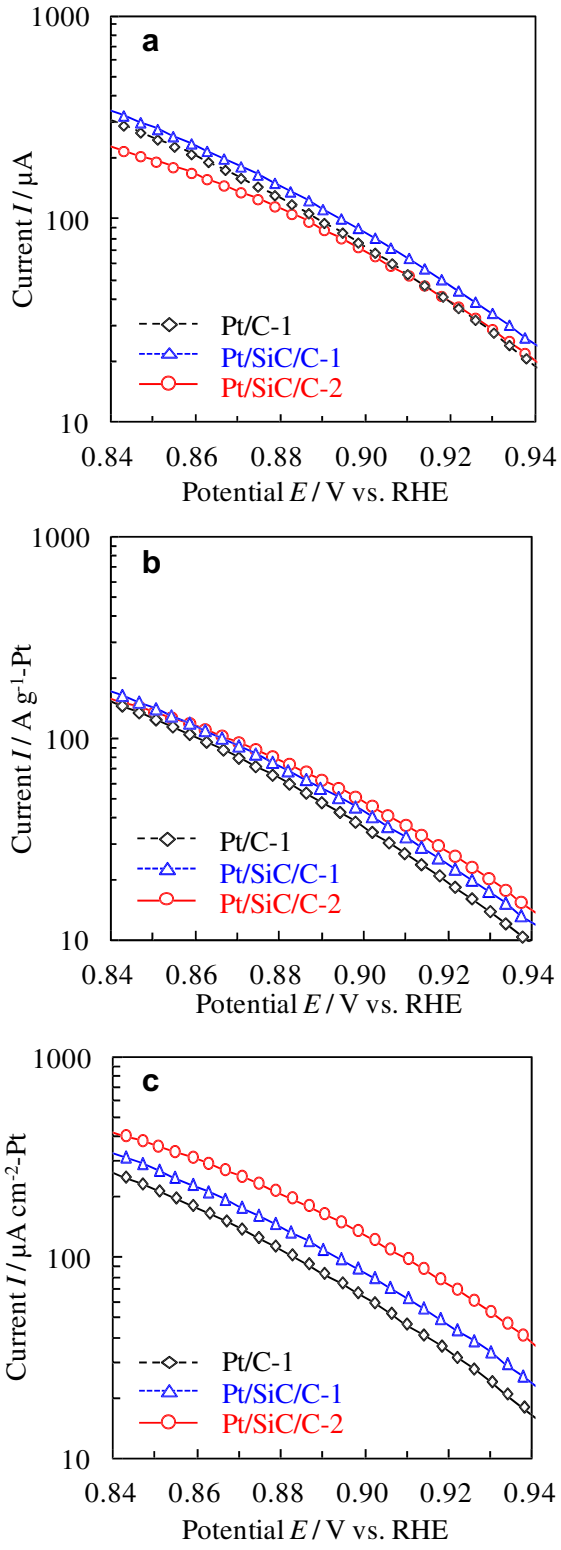

Fig. 7. Oxygen reduction currents (a) not normalized, (b) normalized to Pt weight, and (c) normalized to Pt surface area for all catalysts in 0.1 mol L^{-1} $HClO_4$ at 308 K.

(2.3 nm), and the crystalline sizes were consisted with the platinum particle sizes observed by STEM.

Cyclic voltammograms of all catalysts are shown in Fig. 6. The currents were normalized to the platinum weight in the catalysts. Typical peaks related to platinum were observed at all the catalysts. The platinum surface areas, which were calculated from the hydrogen adsorption and desorption peaks, are listed in Table 2. The platinum surface area of the catalysts decreased in the order of Pt/C-1, Pt/SiC/C-1, and Pt/SiC/C-2. The area of Pt/SiC/C-2 (34 m^2 g^{-1}) was about half that of Pt/C-1 (62 m^2 g^{-1}). This was due to the difference in the platinum particle size of each catalyst.

3.3. Oxygen reduction activity of catalysts

The oxygen-reduction currents of the catalysts are plotted in Fig. 7(a). The currents normalized to the platinum weight (mass activity) and platinum surface area (specific activity) were also plotted in Fig. 7(b) and (c), respectively. The mass activities and specific activities at 0.9 V of all catalysts are listed in Table 2. All catalysts had almost the same mass activity. On the contrary, the specific activities were different in each catalyst. The specific activity of the catalysts with SiC was higher than that without SiC, and the current of Pt/SiC/C-2 was twice as large as that of Pt/C-1. The reason for the high specific activity of Pt/SiC/C-2 is probably due to the effect of SiC. Ceramic supports have been reported to enhance the oxygen-reduction activity of thin platinum film compared to a carbon support [28]. The carbon support spreads a lattice constant of thin platinum film on it. On the other hand, the ceramic supports maintain the lattice constant of thin platinum film as that of bulk platinum. The platinum-lattice expansion, which is observed on the carbon support, results in lower oxygen-reduction activity. In this work, platinum nanoparticles were placed on the carbon black or the SiC. The ratio of platinum nanoparticles on the SiC to those on the carbon black could increase in order from Pt/C-1, Pt/SiC/C-1, and Pt/SiC/C-2. The platinum lattice constants, which were calculated from the diffraction angles of Pt (111) in Fig. 5, of Pt/C-1, Pt/SiC/C-1, and Pt/SiC/C-2 were 0.3930, 0.3927, and 0.3922 nm, respectively. The platinum lattice of Pt/C-1 expanded more than that of normal platinum powder (0.3923 nm: ICDD), whereas that of Pt/SiC-2/C was coincident with that of normal platinum. Therefore, the Pt/SiC/C-2 demonstrated the highest specific activity. Another reason for this was ascribed to the effect of platinum particle size. The specific activity of platinum nanoparticles decreases as their size decreases [34]. The large size of platinum particles in Pt/SiC/C-2 might result in the highest specific activity. Further investigation is needed to clarify the reason for the high specific activity in the catalyst with SiC by preparing catalysts with the same size of platinum particles.

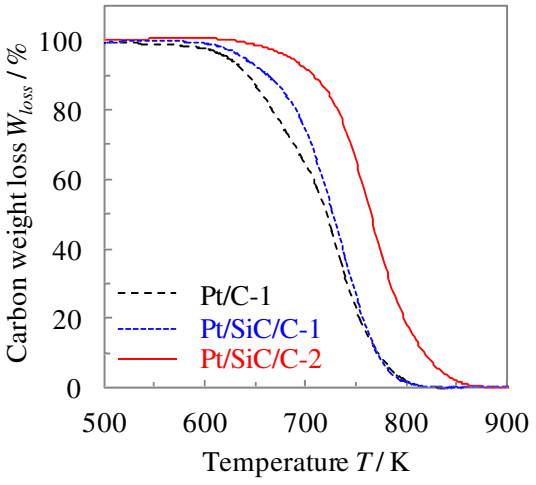

Fig. 8. Carbon weight loss for all catalysts measured by TG analyzer in air at heating rate of 10 K min^{-1}.

3.4. Stability of catalysts

The stability of the catalysts was examined by analyzing the carbon weight loss using a TG analyzer in an oxidation atmosphere of air. The carbon weight losses of the catalysts are shown in Fig. 8. The carbon weight of Pt/C-1 was reduced from 600 K. However, the carbon weight of Pt/SiC/C-1 and Pt/SiC-2 remained at a higher temperature than that of Pt/C-1. The respective temperatures at which the carbon weight was reduced to 80% were 682 K, 705 K, and 749 K for Pt/C-1, Pt/SiC/C-1, and Pt/SiC/C-2. These results revealed that the stability of the catalysts increased by coating the carbon black with SiC. The stability of the catalysts was also evaluated by the potential-cycling test between 1.0 and 1.5 V for a total of 2000 cycles. In this high potential region, carbon supports gradually oxidized [8,10]. The cyclic voltammograms of Pt/C-1 and Pt/SiC/C-2, which was obtained during the potential-cycling test, were shown in Fig. 9(a) and (b), respectively. The hydrogen adsorption and desorption peak of the two catalysts decreased with increasing the cycling number, indicating the platinum surface area of the two catalysts decreased during the potential-cycling test. This result is mainly due to the corrosion of the carbon supports and subsequent agglomeration of platinum nanoparticles. The surface area of the catalysts was shown as a function of the cycling number in Fig. 9(c). The surface area loss of Pt/SiC/C-2 was slower than that of Pt/C-1, suggesting the electrochemical stability of the catalysts increased by coating the carbon black with SiC. Platinum nanoparticles enhance the corrosion of carbon supports by their catalytic effect [6–8]. However, in the Pt/SiC/C-1 and Pt/SiC/C-2, many platinum nanoparticles were located on the SiC instead of carbon black. The SiC suppressed carbon oxidation, which caused the platinum nanoparticles. The SiC/C is therefore a promising support material for highly stable cathode catalysts.

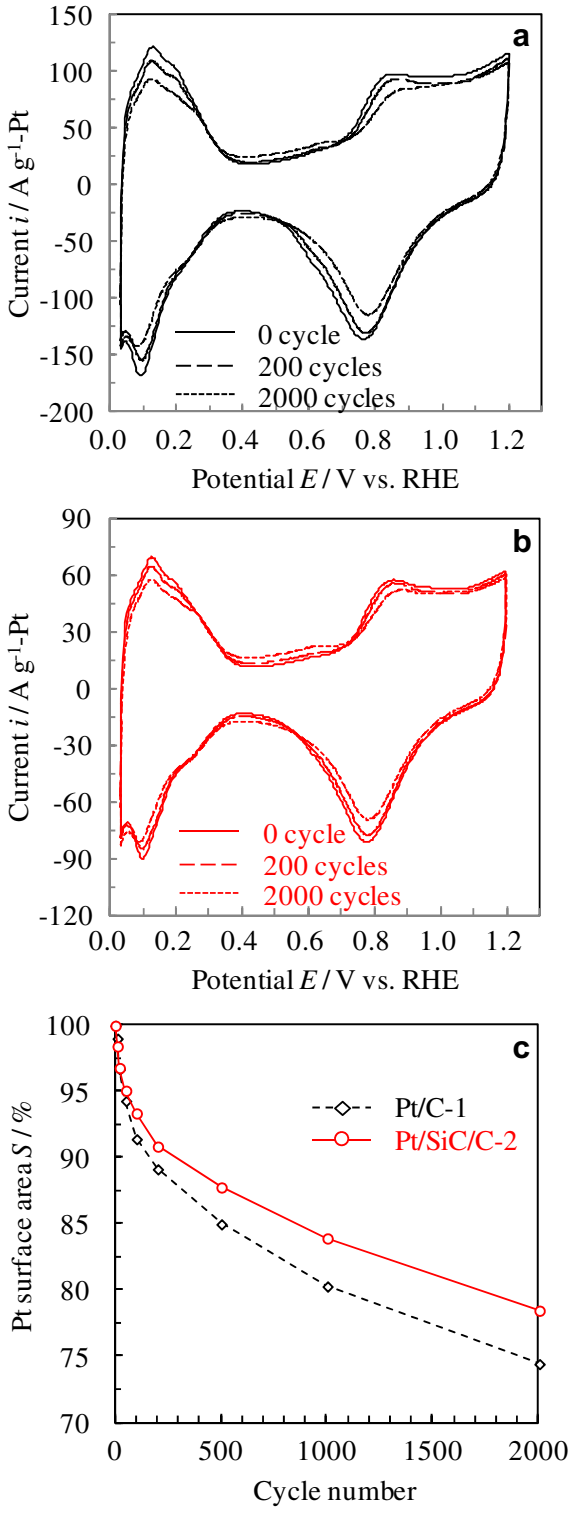

Fig. 9. Cyclic voltammograms obtained in 0.1 mol L^{-1} $HClO_4$ at 337 K of (a) Pt/C-1 and (b) Pt/SiC/C-2 after 0, 200, and 2000 times of potential cycling (1.0–1.5 V), and (c) Pt surface area as a function of potential-cycling number.

4. Conclusion

We prepared SiC-coated carbon blacks (SiC/C) as a support material for cathode catalysts with high stability against oxidation. The SiC/C was synthesized by pyrolyzing PCS on carbon black. An STEM-EDX image of SiC/C revealed that the SiC layer coating the carbon black was less than 10 nm thick. The XPS results indicated that the PCS was clearly pyrolyzed into SiC, and it was partially oxidized. Although the electrical resistance of SiC/C increased with the amount of SiC, the value was of the same order as the carbon black used as a core material of the SiC/C. The platinum-deposited SiC/C (Pt/SiC/C) was synthesized using electroless plating in order to investigate the oxygen reduction activity and stability of the catalysts. The electrochemical measurement showed that the specific activity of Pt/SiC/C was higher than that of Pt/C. The TG analysis in an oxidation atmosphere and the potential-cycling test revealed that the stability of Pt/SiC/C was also higher than that of Pt/C. These results indicate that SiC/C is a very promising support material for cathode catalysts in polymer electrolyte fuel cells.

Acknowledgements

This work was partly supported by The New Energy and Industrial Technology Development Organization (NEDO), Japan.

References

[1] X. Cheng, L. Chen, C. Peng, Z. Chen, Y. Zhang, Q. Fan, J. Electrochem. Soc. 151 (2004) A48–A52.
[2] J. Xie, D.L. Wood III, K.L. More, P. Atanassov, R.L. Borup, J. Electrochem. Soc. 152 (2005) A1011–A1020.
[3] Y. Shao, G. Yin, Y. Gao, P. Shi, J. Electrochem. Soc. 153 (2006) A1093–A1097.
[4] K. Kinoshita, J.A.S. Bett, Carbon 11 (1973) 405–411.
[5] K.H. Kangasniemi, D.A. Condit, T.D. Jarvi, J. Electrochem. Soc. 151 (2004) E125–E132.
[6] J. Willsau, J. Heitbaum, J. Electroanal. Chem. 161 (1984) 93–101.
[7] L.M. Roen, C.H. Paik, T.D. Jarvi, Electrochem. Solid-State Lett. 7 (2004) A19–A22.
[8] Z. Siroma, K. Ishii, K. Yasuda, M. Inaba, A. Tasaka, Electrochem. Commun. 7 (2005) 1153–1156.

[9] L.M. Vračar, N.V. Krstajić, V.R. Radmilović, M.M. Jakšic, J. Electroanal. Chem. 587 (2006) 99–107.
[10] T. Ioroi, H. Senoh, S. Yamazaki, Z. Siroma, N. Fujiwara, K. Yasuda, J. Electrochem. Soc. 155 (2008) B321–B326.
[11] S.H. Kang, T.-Y. Jeon, H.-S. Kim, Y.-E. Sung, W.H. Smyrl, J. Electrochem. Soc. 155 (2008) B1058–B1065.
[12] S.-Y. Huang, P. Ganesan, B.N. Popov, Appl. Catal. B Environ. 102 (2011) 71–77.
[13] M. Wesselmark, B. Wickman, C. Lagergren, G. Lindbergh, Electrochim. Acta 55 (2010) 7590–7596.
[14] K.-W. Park, K.-S. Soel, Electrochem. Commun. 9 (2007) 2256–2260.
[15] T.B. Do, M. Cai, M.S. Ruthkosky, T.E. Moylan, Electrochim. Acta 55 (2010) 8013–8017.
[16] K. Sasaki, L. Zhang, R.R. Adzic, Phys. Chem. Chem. Phys. 10 (2008) 159–167.
[17] M. Nakada, A. Ishihara, S. Mitsushima, N. Kamiya, K. Ota, Electrochem. Solid-State Lett. 10 (2007) F1–F4.
[18] A. Masao, S. Noda, F. Takasaki, K. Ito, K. Sasaki, Electrochem. Solid-State Lett. 12 (2009) B119–B122.
[19] O.A. Balturina, Y. Garsany, T.J. Zega, R.M. Stroud, T. Schull, K.E. Swider-Lyons, J. Electrochem. Soc. 155 (2008) B1314–B1321.
[20] P.J. Kulesza, B. Grzybowska, M.A. Malik, M.T. Galkowski, J. Electrochem. Soc. 144 (1997) 1911–1917.
[21] H. Chhina, S. Campbell, O. Kesler, J. Electrochem. Soc. 154 (2007) B533–B539.
[22] B. Avasarala, T. Murray, W. Li, P. Haldar, J. Mater. Chem. 19 (2009) 1803–1805.
[23] K. Kakinuma, Y. Wakasugi, M. Uchida, T. Kamino, H. Uchida, M. Watanabe, Electrochemistry 79 (2011) 399–403.
[24] H. Chhina, S. Campbell, O. Kesler, J. Power Sources 164 (2007) 431–440.
[25] H. Lv, S. Mu, N. Cheng, M. Pan, Appl. Catal. B Environ. 100 (2010) 190–195.
[26] R.K. Gupta, R. Mishra, K. Mukhopadhyay, R.K. iwari, A. Ranjan, A.K. Saxena, Silicon 1 (2009) 125–129.
[27] M. Luo, Y. Li, S. Jin, S. Sang, L. Zhao, Ceram. Int. 37 (2011) 3055–3062.
[28] S. Suzuki, T. Onodera, J. Kawaji, T. Mizukami, K. Yamaga, Appl. Catal. A Gen. 427–428 (2012) 92–97.
[29] P. Colombo, J. Am. Ceram. Soc. 80 (1997) 2333–2340.
[30] S. Suzuki, Y. Ohbu, T. Mizukami, Y. Takamori, M. Morishima, H. Daimon, M. Hiratani, J. Electrochem. Soc. 156 (2009) B27–B31.
[31] T. Onodera, S. Suzuki, Y. Takamori, H. Daimon, Appl. Catal. A Gen. 379 (2010) 69–76.
[32] T.J. Schmidt, H.A. Gasteiger, G.D. Stab, P.M. Urban, D.M. Kolb, R.J. Behm, J. Electrochem. Soc. 145 (1998) 2354–2358.
[33] B.P. Swain, Surf. Coat. Technol. 201 (2006) 1589–1593.
[34] Y. Takasu, N. Ohashi, X.-G. Zhang, Y. Murakami, H. Minagawa, S. Sato, K. Yahikozawa, Electrochim. Acta 41 (1996) 2595–2600.